ESTIMATING CELING HEIGHT NEAR THE SOUTH POLE USING VISIBLE INFRARED IMAGING RADIOMETER SUITE (VIIRS) CHANNEL 4 BRIGHTNESS TEMPERATURE: A STATISTICAL APPROACH

Jeffrey D. Fournier[1,2] and Matthew A. Lazzara[3,4]

[1]Naval Information Warfare Center (NIWC), Atlantic - Polar Programs (NPP)

[2]DIGITALiBiz LLC, North Charleston, SC

[3]Antarctic Meteorological Research and Data Center, Space Science and Engineering Center, University of Wisconsin-Madison, Madison, WI

[4]Department of Physical Sciences, School of Engineering, Science, and Mathematics, Madison Area Technical College, Madison, WI

1. INTRODUCTION

Accurately observed and forecast cloud ceilings are an important component of safe aviation operations. A ceiling occurs when at least 5/8 of the ground observer's celestial dome is covered by clouds. Sky cover is cumulative from the lowest cloud layer upward. The lowest layer to reach a total of 5/8 coverage is defined as the ceiling height (FMH1, 2019). Ceiling heights can be measured by ceilometers or manually estimated by observers.

Some pilots servicing the Amundsen-Scott South Pole Station must operate within Visual Flight Rules (VFR). For sky conditions, VFR pilots require either no cloud ceiling, or a ceiling height at least 1,000 ft AGL. Pilots operating in ceilings below 1,000 ft AGL must be able to rely exclusively on special navigational instruments. They are certified to fly under Instrument Flight Rules (IFR).

Marginal VFR (MVFR) conditions also command attention from pilots. The ceiling heights in this category range from 1,000 ft to 2,900 ft AGL. The closer the ceiling gets to 1,000 ft AGL, the more wary a VFR pilot should be about attempting a flight.

The South Pole has the only operational ceilometer within at least 1-thousand kilometers of the station. Compared to a human observer, a single ceilometer has a small field of view, both in the horizontal and vertical dimensions (Wagner and Kleiss, 2016). Observers must estimate distant cloud bases and amounts outside of the narrow ceilometer range. Such observations can be prone to significant error, as they are made amidst the vast expanse of nearly featureless, white terrain surrounding the South Pole.

Satellite imagery within the visible and IR wavelengths can be used to estimate ceiling heights. However, shallow low clouds sometimes lack sufficient contrast with the surface to be easily seen (Figures 1a-1b). Higher-level clouds, even thin layers, can sometimes mask lower clouds (Figures 2a-2b).

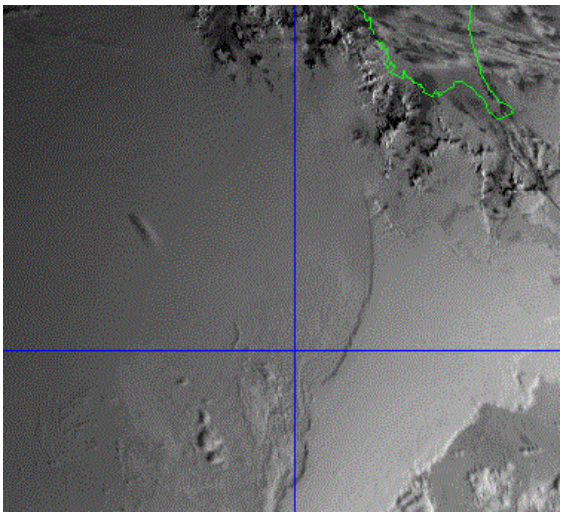

Figure 1a. 1701 UTC 13 FEB 2022 visible channel from Meteorological Operational (MetOp) Satellite. 900 ft ceiling at South Pole (blue cross) at 1650 UTC.

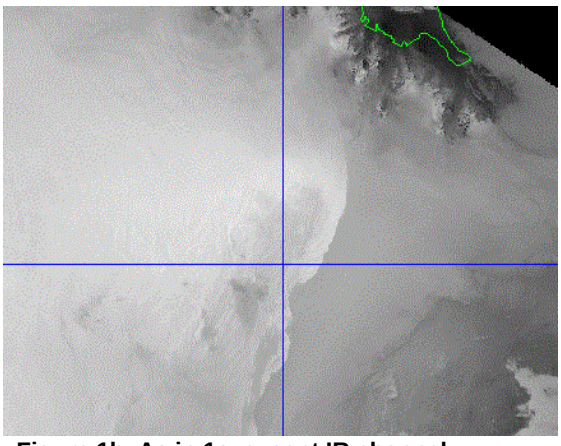

. **Figure 1b. As in 1a, except IR channel.**

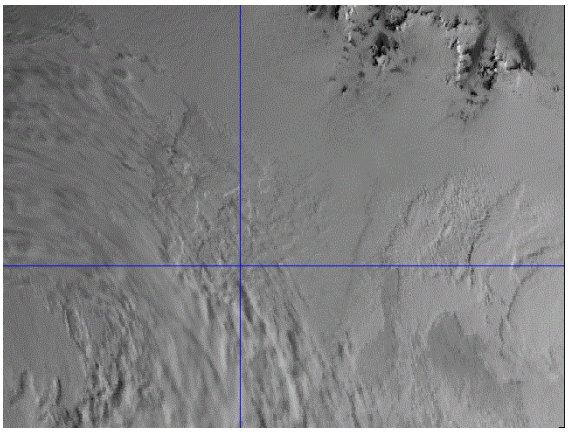

Figure 2a. 1657 UTC 19 JAN visible from Terra Moderate-Resolution Imaging Spectroradiometer (MODIS). 1,200 ft ceiling at 1650 UTC.

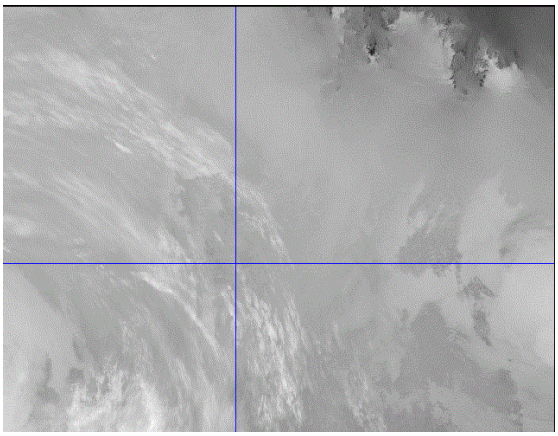

Figure 2b. 1724 UTC 19 JAN IR from NOAA-20 VIIRS. 1,200 ft ceiling at 1650 UTC.

NPP forecasters recently obtained routine access to data from the VIIRS aboard the Suomi National Polar-orbiting Partnership (S-NPP) and National Oceanic and Atmospheric Administration (NOAA-20) polar-orbiting weather satellites. This includes channel I4 data. This fine resolution (375 m) channel covers “medium-wave” wavelengths centered at 3.74 µm.

Brightness temperature data from this channel are plotted using a gray scale which is opposite the IR scale used in most weather satellite imagery. Cold values are depicted as dark gray, while warm values appear as bright gray (Figure 3).

NPP forecasters have gravitated toward this product during the long daylight hours of the austral summer. Channel 4 imagery generally offers greater contrast between relatively thin, low clouds and the surface (Figure 3 vs. Figures 1a and lb). Such clouds can

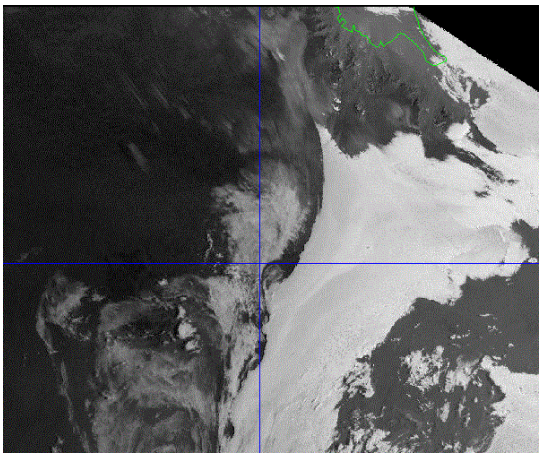

Figure 3. 1704 UTC 13 FEB channel 4 from NOAA-20 VIIRS.

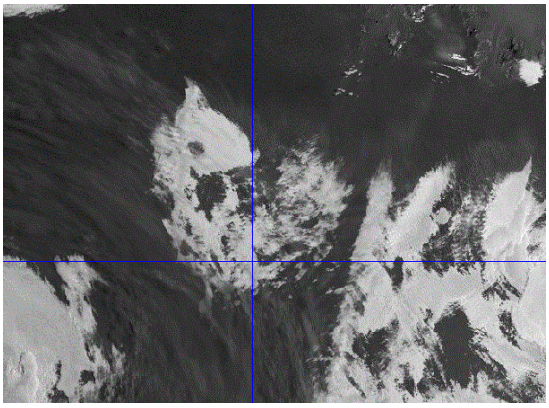

Figure 4. As in 3, except 1724 UTC 19.

even appear through thin cirrostratus (Figure 4 vs. Figures 2a and 2b).

The temperature measured at the top of the low cloud layer at the South Pole on 13 FEB was approximately -35^{o} C (Figure 5). However, the mean brightness temperature from the channel 4 image was 5^{o} C. The very small ice crystals in the low stratus reflect insolation well, leading to the warmer temperature measured by VIIRS in channel 4 (CIMMS, ABI Band 7 Quick Guide). The combination of emitted longwave radiation and solar reflection of the snowy surface remains significantly colder than the clouds when measured at the 3.74 µm wavelength (Trepte, 2002).

Although channel 4 imagery is an effective tool for detecting low clouds, it offers no obvious clues about the corresponding cloud bases. This work explores the possible statistical correlation between the brightness temperature of channel 4 imagery and the observed ceiling height at the South Pole.

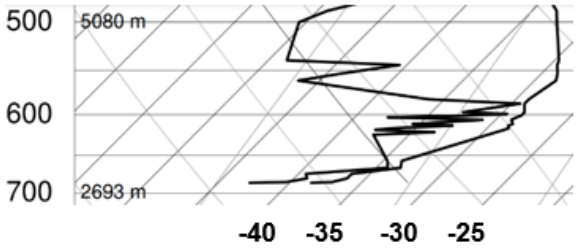

Figure 5. Skew-T/Log-P observation from South Pole valid 00 UTC 14 FEB. Courtesy of University of Wyoming.

2. METHODS

Automatically generated Meteorological Aerodrome Reports (METAR) and Special observations (SPECI) from the South Pole were not disseminated during the 2021-2022 operational season. (METAR and SPECI are the standard international reports used to disseminate ceiling information and other weather data measured from the surface). The manually generated METARs and SPECIs were rather sporadic, driven largely by aircraft operations. The South Pole observers did have access to their automated observing system, including its ceilometer.

TeraScan® is NPP's operational platform for satellite data retrieval and interrogation. It uses a proprietary TDF format. Limited real-time imagery archival in this system prevented examining satellite data from the period prior to 19 January.

Channel 4 imagery from NOAA-20 and S-NPP VIIRS was examined from 1306 UTC 19 January 2022 through 1037 UTC 28 February 2022. For an image to be included, the satellite pass had to have a valid time within 20 minutes of the surface observation. The mean time difference between the satellite and surface observation was 10 minutes and 36 seconds. Both METARs (taken at 10 minutes till the top of the hour) and SPECIs (taken when certain weather criteria are met) were used. Observations with missing ceiling height due to technical failures were excluded.

Total sky cover is one of the most subjective parts of a surface observation. Observers must estimate the total cloud amount covering the celestial dome (FMH1, 2019). They must also determine if and at what height a cloud ceiling exists. South Pole observers use a ceilometer to help measure cloud bases. A ceilometer can accurately measure the distance between the ground and a cloud base, provided the cloud is within the limited range of the sensor.

Automated observing platforms like the one used at the South Pole use a time averaging algorithm to help mitigate the discrepancy between the human observer's wide field of view and the ceilometer's narrow field of view (Wagner and Kleiss. 2016). In doing this, the ceilometer and algorithm become a means for the automated system to estimate total sky cover, including the existence of ceilings.

Wagner and Kleiss (2016) found that these systems work well in steady state sky conditions. However, it is often too slow to adapt to what the human observer sees when sky conditions change rapidly. Observers must rely on their best judgement to accurately describe the sky conditions in the interest of safe aircraft operations.

To help ensure the observed sky condition correctly matches the corresponding satellite data, no large brightness temperature gradient was permitted over the South Pole. This restriction is meant to prevent the ambiguous cases which occur with rapidly changing sky conditions at observation times. In such cases, the time lag between the surface and satellite observation could result in unwanted discontinuity between the two observations.

For each potential pairing of a satellite image with a surface observation, the channel 4 brightness temperature was measured for the 4 pixels centered at the South Pole. These pixels form a 2.2 x 2.2 km square (Figure 6). This area is closer to the area covered by a surface observer's celestial dome than that of a single pixel.

If a brightness temperature difference of 10 K or greater was measured between any of the 4 pixels of the square, that image and corresponding ceiling height were not included in this study. This 10 K threshold is admittedly arbitrary. Otherwise, the average of the 4 pixels is the brightness temperature used to pair with the surface observation. A possible disadvantage of this method is the potential for smearing of the brightness temperatures.

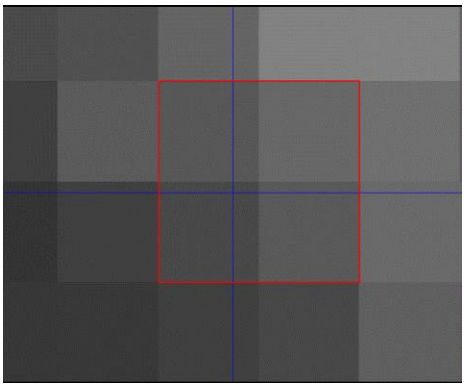

Figure 6. Maximum zoom over South Pole. The average brightness temperature is calculated using the brightness temperature of each of the 4 pixels within the 2.2 x 2.2 km square.

There were multiple instances when ceilings did not occur. This would result in those ceiling heights being unbounded and those cases being excluded. To keep the data set as large as possible, these occurrences were assigned a value of a 10,000 ft AGL ceiling height. Additionally, 10,000 ft was set as the upper limit for all reported ceilings. Ceilings at or above this level are typically unimportant to aviators. Also, observations at these higher levels become less reliable and less precise (FMH1, 2019) than lower cloud bases.

3. RESULTS

The 123 cases which fit these criteria were examined in Excel using the *Analysis ToolPak* Add-in. The correlation coefficient is -0.68 and P-value is less than 0.001. The R^2 value of 0.46 indicates too much variance to use a regression model to consistently estimate ceiling heights based on brightness temperatures (Figure 7).

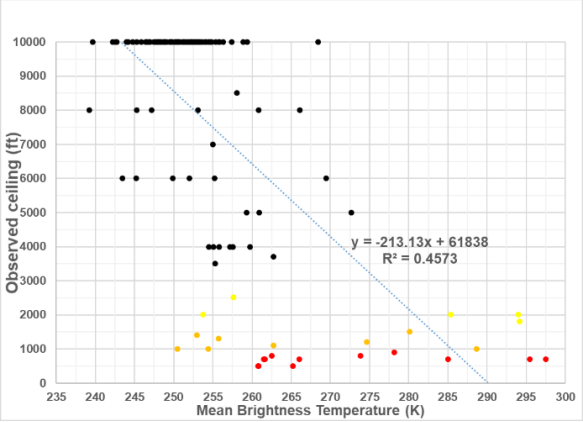

Figure 7. Scatter plot of ceiling height vs. mean brightness temperatures at South Pole from 19 JAN 2022 – 28 FEB 2022. Red dots are observed IFR ceilings, orange dots are low (MVFR), yellow dots are higher MVFR, and black dots are VFR. Also shown are regression line with equation.

However, there appears to be enough clustering of data points and negative correlation to suggest some general forecasting guidelines. For example, all 12 IFR ceilings occur when the mean brightness temperature exceeds 260 K. In only 6% of the cases are VFR ceilings reported with a brightness temperature greater than 260 K.

69% of the MVFR cases occur when the brightness temperature exceeds 255 K. Only 20% of the cases have VFR ceilings with a brightness temperature greater than 255 K. This discriminator is not as sharp as the previous one, as it fails to catch all MVFR cases and has a higher false alarm rate.

The 255 K brightness temperature also appears to have utility in separating ceilings of 10,000 ft AGL from ceilings below 10,000 ft AGL. (Recall that for this study, 10,000 ft AGL includes observations with no ceilings and ceilings exceeding 10,000 ft AGL). 89% of the cases with 10,000 ft ceilings occur when the brightness temperature is below 255 K.

All 13 observed MVFR ceilings occur with a brightness temperature greater than 250 K. However, the number of VFR ceilings matching this threshold swells to 58, increasing the false alarm rate to an undesirable 47%.

There is significant overlap of IFR and MVFR ceilings, as they relate to brightness temperature. For brightness temperatures above 260 K, which contain all IFR instances, there are also 7 MVFR occurrences. That is 54% of the total instances of MVFR ceiling heights.

The peak daily sun elevation angle during this study ranged from 21º on 19 January to 8º in late February (data courtesy of timeanddate.com). The crudely estimated minimum brightness temperature in the vicinity of the South Pole ranged from approximately 245 K in late January, to 235 K by mid-February. This seems to confirm the importance of insolation at this wavelength.

Because of this channel's sensitivity to insolation, consideration was given to cutting off the data on 17 February or parsing the data pairs into shorter time periods. The shorter period from 19 January through 17 February yields a correlation coefficient of -0.79, R^2 value is 0.63, and P-value less than 0.001.

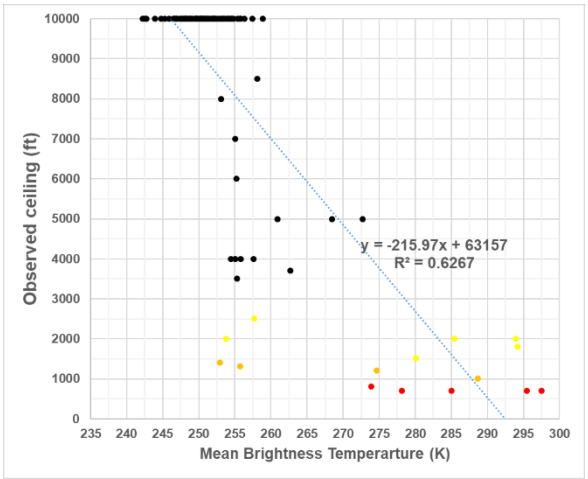

Figure 8. As in Figure 7, except 19 JAN – 17 FEB 2022.

Despite these improvements, there remains too much variance to use this regression equation in operational

forecasting (Figure 8). Perhaps a more pressing concern with this approach is the number of IFR ceiling heights being reduced from 12 to only 5. IFR ceilings are the most important data points of this study. Sacrificing these data for the modest improvements in the regression equation appears to be an inadequate tradeoff.

4. CONCLUSIONS

This work examines the negative correlation between observed cloud ceiling height and VIIRS channel 4 brightness temperature at the South Pole. Archived satellite imagery and surface observations from the late austral summer of 2022 are examined.

For an observation pairing to be included, the satellite pass had to be within 20 minutes of the surface observation. Additionally, only cases with brightness temperature gradients of 10 K or less over the South Pole were considered. Having met these criteria, the average channel 4 brightness temperature was calculated for the 2.2 x 2.2 km square centered at the South Pole. 123 cases met these criteria.

There is a negative correlation (-0.68 coefficient) between the channel 4 mean brightness temperature and observed cloud ceiling height at the South Pole. The R^2 value of 0.46 shows too much variance for an operational linear regression model. There is, however, enough clustering of data points to suggest 3 guidelines to assist forecasters in determining cloud ceilings based on channel 4 imagery. (T is VIIRS channel 4 mean brightness temperature):

1. If T > 260 K, forecast ceilings from 500 ft to 900 ft AGL (IFR)
2. If 255 K < T < 261 K, forecast ceilings from 1,000 to 2,500 ft AGL (MVFR)
3. If T < 255 K , forecast ceilings of at least 10,000 ft AGL (or no ceilings).

There are potential concerns with these guidelines. Among these are the limited sample size of IFR ceilings. Only 12 of the 123 cases are IFR ceiling heights. Of these IFR cases, none are below 500 ft AGL. Ceiling heights below 500 ft AGL do occasionally occur. Such ceilings can even limit IFR operations.

There is considerable overlap of IFR and MVFR ceiling heights for brightness temperatures exceeding 260 K. Following the first guideline is likely to lead to IFR ceiling heights being forecast too frequently.

The VIIRS measurements near the 3.74 µm wavelength remain sensitive to reflected solar radiation. The best correlation between brightness temperature and ceiling height occurred while the peak daily sun angle was 13° or greater, which is approximately 26 October through 17 February. (Note that this work does not include data prior to 19 January). Extra caution is urged when examining channel 4 imagery outside this date range. During these fringe periods, the use of these guidelines should be confined to those portions of the day during the highest sun angle.

The plan is for this database to grow over the next few austral summers. Through this expanding data set, the authors hope to refine these forecast guidelines. Additional investigation of events such as this could be conducted via more complete archives of South Pole observations from the AMRDC Data Repository and satellite imagery via the formal archive of VIIRS from S-NPP and NOAA-20 from NOAA's Comprehensive Large Array-data Stewardship System (CLASS). However, as noted, this is an investigation of what was available to forecasters at the time, revealing the limits of what can be done with limited observational datasets, In real-time.

5. ACKNOWLEDGEMENTS

The authors wish to thank the support of the Office of Polar Programs, National Science Foundation grant # 1951720 abd 1951603.

6. REFERENCES

Cooperative Institute for Meteorological Satellite Studies (CIMSS), Space Science & Engineering Center (SSEC), and University of Wisconsin-Madison 2022: ABI Band 7 (3.9 µm) *Quick Guide*, accessed 6 July 2022, http://cimss.ssec.wisc.edu/goes/OCLOFactSheetPDFs/ABIQuickGuide_Band07.pdf

Office of the Federal Coordinator for Meteorological Services and Supporting Research, 2019: Federal Meteorological Handbook No.1 Surface Weather Observations and Reports (FCM-H1-2019). https://www.icams-portal.gov/resources/ofcm/fmh/FMH1/fmh1_2019.pdf

Oolman, L., 2022: 00 UTC 14 FEB 2022 RAOB from Amundsen-Scott base at South Pole. University of Wyoming College of Engineering Department of Atmospheric Science Soundings. https://weather.uwyo.edu/upperair/sounding.html

Thorsen, S., 1998: timeanddate.com, accessed 6 July 2022, https://www.timeanddate.com/sun/antarctica/

Trepte, Q., Minnis, P., Arduini, R., 2002: Daytime and nighttime polar cloud and snow identification using MODIS data. *SPIE 3rd International Asia-Pacific Environmental Remote Sensing Symposium 2002: Remote Sensing of the Atmosphere, Ocean,*

Environment, and Space, Hangzhou, China October 23-27, 2002. https://www.ametsoc.org/index.cfm/ams/publications/author-information/formatting-and-manuscript-components/references/

Wagner, T. and Kleiss, Jessica, 2016: Error Characteristics of Ceilometer-Based Observations of Cloud Amounts, *J. Atmos. Oceanic Technol*, **33**, 1557-1567, https://journals.ametsoc.org/view/journals/atot/33/7/jtech-d-15-0258_1.xml

.